Green Chemistry

PAPER

View Article Online
View Journal | View Issue

Cite this: *Green Chem.*, 2025, **27**, 12421

Sustainable silica microcapsules

O. Norvilaite,[a] C. Lindsay,[b] M. J. Rymaruk,[b] P. Taylor[b] and S. P. Armes *[a]

Received 30th June 2025,
Accepted 8th September 2025

DOI: 10.1039/d5gc03298a

rsc.li/greenchem

Microencapsulation is a critical technology for a wide range of commercial applications, including drug delivery, home and personal care products, fragrance release, agrochemicals, food manufacture, energy storage and self-healing materials. In many cases, highly crosslinked polymer microcapsules are utilized, which are now regarded as microplastic pollutants. Herein we report a new route to sustainable micrometer-sized silica microcapsules based on the judicious use of a binary mixture of chitosan and hydroxypropyl cellulose. This synergistic emulsifier system enables the preparation of oil-in-water emulsions with a mean droplet diameter of approximately 5–10 μm. Chitosan adsorption at the oil–water interface confers cationic surface charge, which directs the surface deposition of environmentally benign silica from the aqueous continuous phase when employing TMOS as a silica precursor. However, the addition of TEOS to the oil phase prior to high-shear homogenization is also required to produce the most robust silica microcapsules. Interestingly, the two biopolymers located within the silica shells confer mechanical flexibility, which may offer an advantage for controlled release applications. The mean silica shell thickness can be varied from 50 to 175 nm, and thermogravimetry analysis of the dried silica microcapsules indicated a mean biopolymer content of around 29% to 38% by mass. Preliminary experiments indicate that substantial release of a model payload (dimethyl phthalate) occurs within 6 h at 20 °C. Thus, these microcapsules are highly porous towards sparingly water-soluble small molecules. On the other hand, they retain a model water-insoluble dye for at least sixteen weeks when stored at 20 °C.

Green foundation

1. Silica microcapsules are a potential replacement for non-degradable polymer-based microcapsules which have been widely used to deliver various agrochemicals over the past forty years by companies such as Syngenta but are now classified as an environmental pollutant (microplastics). In contrast, silica is a naturally-occurring, environmentally benign material.
2. Micron-sized silica microcapsules are prepared under mild conditions at relatively high solids using a wholly aqueous formulation involving cheap, commercially available reagents.
3. Silica microcapsules that retain sparingly water-soluble compounds for longer periods would be a useful future advance. In principle, this could be achieved by targeting thicker silica shells. It would also be useful to be able to prepare such silica microcapsules at higher solids. Nevertheless, our new synthetic route is sufficiently promising for the industrial sponsor of this study (Syngenta) to file a patent application to protect the associated IP.

Introduction

Microencapsulation is a critical technology for a wide range of commercial applications, including drug delivery, home and personal care products, fragrance release, agrochemicals, food manufacture, energy storage and self-healing materials.[1–20] In some cases, slow sustained release of the encapsulated active is sought, which requires a relatively thick shell layer of low permeability.[20–23] On the other hand, rapid release may be desirable, which may involve using an erodible or chemically-responsive shell.[1,11,14,18] Finally, permanent retention of the active material may be needed, as in the case of wax-loaded microcapsules for temperature regulation and/or energy storage.[24–28]

Over the past few decades, there has been a concerted effort to design various types of polymer-based microcapsules. This can be achieved by either interfacial copolymerization[29–36] or physical methods such as controlled solvent evaporation to deposit a homopolymer shell at an oil/water interface.[21,37–39] However, non-degradable polymer microcapsules derived from vinyl monomers are now classified as microplastic pollutants and are subject to stringent legislation regarding their use.[40] Thus many industrial products and processes need to be reformulated by developing more environmentally-friendly

[a]*Dainton Building, School of Mathematical and Physical Sciences, University of Sheffield, Brook Hill, Sheffield, South Yorkshire, S3 7HF, UK.*
E-mail: s.p.armes@sheffield.ac.uk
[b]*Syngenta, Jealott's Hill International Research Centre, Bracknell, Berkshire, RG42 6EY, UK*

microcapsules based on either biodegradable polymers or naturally-derived inorganic materials such as calcium carbonate,[19,41] clays[42–44] or silica.[23,45–52]

Silica-based microcapsules are particularly relevant to the present study. There are three soluble silica precursors commonly used in the literature: tetraethyl orthosilicate (TEOS), tetramethyl orthosilicate (TMOS), and sodium silicate. The optimum mean microcapsule diameter depends on the intended application. For example, relatively large microcapsules are required for fragrance release in fabric conditioner formulations to ensure efficient deposition onto textile fibers.[53] On the other hand, much smaller (typically submicron-sized) microcapsules are usually desired for drug delivery[5,54,55] or energy storage applications,[24,56,57] whereas microcapsules of intermediate size (*ca.* 5–10 μm diameter) are often preferred for agrochemical formulations[14,33,49,58] or for the controlled release of fragrances or flavors.[16,50,51,59]

Herein we report a new, potentially scalable route to micrometer-sized sustainable silica microcapsules. First, two widely available biopolymers, chitosan and hydroxypropyl cellulose, are used to prepare an oil-in-water emulsion *via* high-shear homogenization at pH 2.1–4.9.[60]

In this formulation, the oil phase comprises Solvesso 200 ND, dimethyl phthalate (DMP) and TEOS. Then TMOS is added to the aqueous continuous phase, and silicification occurs on both sides of the oil–water interface to produce silica microcapsules at 20 °C (see Scheme 1).

^{29}Si NMR spectroscopy is used to study the kinetics of silicification, and the resulting silica microcapsules are evaluated using a wide range of techniques, including optical and fluorescence microscopy, laser diffraction, aqueous electrophoresis, thermogravimetry, FT-IR spectroscopy and scanning electron microscopy. Finally, preliminary release studies are conducted using UV spectroscopy to monitor the diffusional release of a sparingly water-soluble model payload (DMP) from the interior of the microcapsules into the aqueous continuous phase.

Experimental

Materials

Low molecular weight chitosan (molecular weight = 50 000–190 000 g mol^{-1}; 75–85% deacetylated) and hydroxypropyl cellulose (HPC; MW = 80 000 g mol^{-1}, 99%) were purchased from Sigma-Aldrich (UK). Tetramethyl orthosilicate 98% (TMOS; 98% purity), tetraethyl orthosilicate (TEOS; 98% reagent grade) and dimethyl phthalate (DMP; 99% purity) were purchased from Sigma-Aldrich (UK). Solvesso 200 ND (ex. ExxonMobil) was provided by Syngenta International (Bracknell, UK). This industrial oil comprises C_{10}–C_{13} hydrocarbons, aromatics and trace naphthalene (<1%). It has a viscosity of 4.4 cS at 20 °C, a density of 0.98 g cm^{-3}, a vapor pressure of less than 1 Pa (0.01 mmHg) at 20 °C, a log p value of 3.80–3.87, and negligible solubility in water. Glacial acetic acid was purchased from VWR (UK). Absolute ethanol (≥99.8%, HPLC grade) was purchased from Fisher (UK). d_4-Acetic acid (99.5 atom % D), DCl (35 wt% in D_2O; ≥99 atom% D), D_2O (99.9 atom % D), hexamethyldisiloxane (HMDS; ≥98.5% purity), chromium(III) acetylacetonate ($Cr(acac)_3$; 97% purity) and Nile Red (for fluorescence microscopy) were purchased from Sigma-Aldrich (UK). d_6-Dimethyl sulfoxide (DMSO; 99.9 atom % D) and d_4-methanol (99.8 atom % D) were purchased from Goss Scientific (Cheshire, UK). Deionized water (pH 6) was used for all experiments.

Preparation of silica microcapsules

The following protocol was used to target silica microcapsules with a mean shell thickness of 100 nm (the equation and assumptions used to calculate the mean silica shell thickness are described in the SI) using a TEOS/TMOS molar ratio of 1.0 at pH 3.8. A 0.89% w/w aqueous solution containing chitosan and HPC was prepared by dissolving 0.020 g of each biopolymer in 0.1 M acetic acid (4.460 g). The oil phase used in

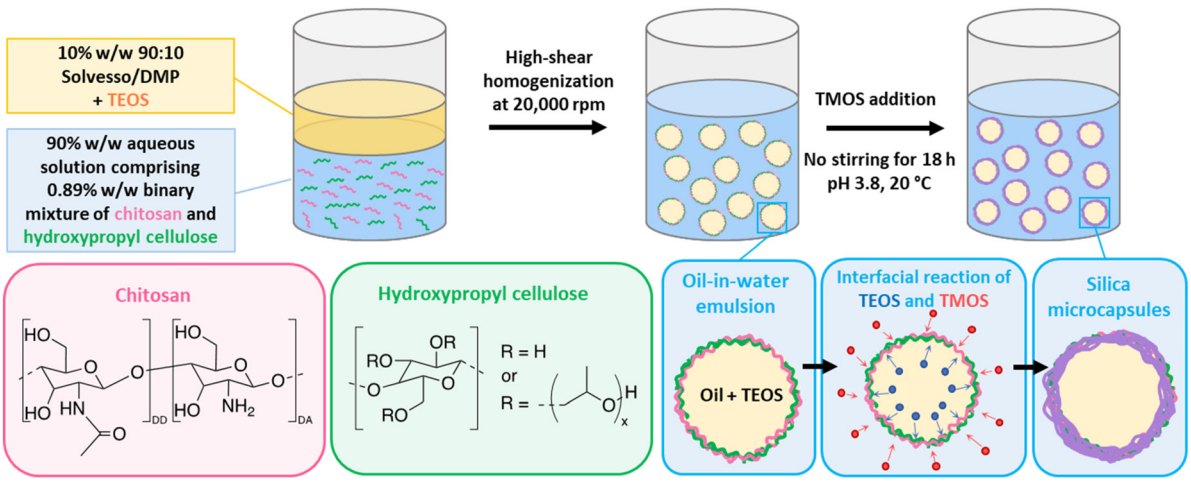

Scheme 1 Synthesis of silica microcapsules *via* silicification of a biopolymer-stabilized oil-in-water emulsion prepared via high-shear homogenization using a binary mixture of TMOS and TEOS.

these experiments comprised 90% w/w Solvesso 200 ND plus 10% w/w dimethyl phthalate (DMP). This oil phase (0.500 g) was placed in a tall 14 mL glass vial containing TEOS (0.2167 g). The weakly acidic aqueous phase was added to form a biphasic mixture, which was homogenized at 20 °C for 2.0 min at 20 000 rpm using an IKA Ultra-Turrax T-18 basic homogenizer equipped with a 10 mm dispersing tool. TMOS (0.1584 g) was added to the resulting emulsion and the vial was gently inverted for 10 s to ensure even mixing before leaving the reaction mixture to stand for 18 h. The silica microcapsules were purified *via* three centrifugation-redispersion (8000 rpm for 10 min using a Beckman Coulter Avanti J-E centrifuge), with each aqueous supernatant being replaced with deionized water adjusted to pH 4.0 using acetic acid. To facilitate some analyses, the silica microcapsules were subjected to further centrifugation-redispersion cycles following the same protocol, except the supernatant was replaced with ethanol. This led to extraction of the oil cores prior to drying in a 40 °C oven for 16 h.

The chitosan/HPC mass ratio was systematically varied by mixing varying proportions of 2.0% w/w stock solutions of chitosan and HPC (prepared at pH 4.0 using 0.1 M acetic acid) followed by dilution with 0.1 M acetic acid as required. For example, preparation of a 0.89% w/w aqueous phase at a chitosan/HPC mass ratio of 0.25 required 2.0% w/w chitosan stock solution (0.445 g), 2.0% w/w HPC stock solution (1.780 g) and 0.1 M acetic acid (2.775 g). The pH of the aqueous phase was adjusted as required by varying the acetic acid concentration. When varying the oil mass fraction, the total biopolymer concentration was fixed at 0.80% w/w of the final emulsion.

Monitoring silicification kinetics *via* ^{29}Si NMR spectroscopy

Chromium(III) acetylacetonate ($Cr(acac)_3$) was used as a paramagnetic relaxation agent (PRA) to enhance the signal intensity and hence reduce the spectrum acquisition time. Empirically, the optimal $Cr(acac)_3$ concentration within the oil phase was found to be 0.02% w/w. An external reference solution was prepared by mixing 0.375% w/w $Cr(acac)_3$ dissolved in d_6-DMSO (0.09 g), hexamethyldisiloxane (HMDS, 0.25 g) and d_4-methanol (1.31 g) to obtain final $Cr(acac)_3$ and HMDS concentrations of 0.02% w/w and 15% w/w, respectively. A coaxial insert with a 2 mm diameter stem was placed in a standard 5 mm NMR tube containing 0.50 mL of the external reference solution.

Rate of release of dimethyl phthalate from silica microcapsules *via* UV spectroscopy

To monitor the rate of DMP release, 1.00 g of a 10% w/w suspension of the silica microcapsules was placed in dialysis tubing (molecular weight cut-off = 8000 g mol^{-1}). The sealed dialysis tubing was immersed in 100 g of weakly acidic aqueous solution (adjusted to pH 4.5) in a glass jar at 20 °C and stirred at 130 rpm. The aqueous continuous phase was periodically sampled and filtered using a 0.20 μm syringe filter into a 1.0 mL quartz cuvette cell. The maximum absorbance of DMP was recorded at 276 nm using an Agilent Cary 60 UV-Visible spectrophotometer. After each measurement, the aqueous solution was returned to the glass jar containing the dialysis tubing to maintain a constant volume. A linear Beer–Lambert calibration curve was constructed *via* successive dilution of an aqueous stock solution of DMP (with DMP concentrations ranging from 10 to 100 ppm). The same protocol was used to determine the rate of release of DMP from the analogous oil-in-water emulsions (*i.e.* prior to silica microcapsule formation).

Characterization techniques

Optical microscopy. Oil-in-water emulsions were imaged using a Cole-Parmer optical microscope equipped with a MoticamBTW camera connected to a computer.

Scanning electron microscopy. SEM images were recorded using an FEI Inspect F50 field emission scanning electron microscope at an acceleration voltage of 10 kV. Samples were prepared by drying dilute aqueous suspensions of silica microcapsules onto silicon wafers. Sample-loaded wafers were mounted onto aluminum stubs using adhesive carbon tabs. Each stub was then sputter-coated to produce a 5 nm gold overlayer, followed by application of silver paint to two edges of the mounted silicon wafers. Given the electrically insulating nature of the silica microcapsules, this protocol is essential to minimize sample charging. Mean silica microcapsule diameters and wall thicknesses were estimated using ImageJ 1.53k software.

Laser diffraction. The initial oil-in-water emulsions and final silica microcapsules were analyzed using a Malvern Mastersizer 3000 instrument equipped with a HeNe laser (λ = 633 nm), a LED blue light source (λ = 470 nm) and a Hydro EV wet dispersion unit operating at 1600 rpm. The volume-average diameter, $D[4,3]$, and surface-average diameter, $D[3,2]$, were determined by averaging over three measurements. The sample cell was rinsed three times with deionized water between measurements to prevent cross-contamination. The refractive index for Solvesso oil (1.60) and silica (1.54) was used for analysis of the oil-in-water emulsions and silica microcapsules, respectively.

Aqueous electrophoresis. Aqueous suspensions of silica microcapsules were diluted to 0.05% w/w using 1 mM KCl as background electrolyte and analyzed using a Malvern Zetasizer Nano ZS instrument. The Smoluchowski approximation was applied to calculate zeta potentials using the Henry equation. The pH of each suspension was monitored using a calibrated pH probe and adjusted as required using either 0.1 M HCl or 0.1 M NaOH. All measurements were performed in triplicate to obtain mean values. The same protocol was used to construct a zeta potential *vs.* pH curve for an oil-in-water emulsion.

^{1}H NMR spectroscopy. Spectra were recorded using a Bruker Avance 400 MHz instrument with D_2O employed as a solvent lock. Each spectrum was averaged over 16 scans and the typical delay time (D_1) was 1 second between each spectrum. Thus the total accumulation time was approximately 1 min per spectrum.

^{29}Si NMR spectroscopy. Spectra were recorded using the same Bruker Avance 400 MHz instrument employing d_4-methanol as the solvent lock. A zgig pulse program involving a 1D sequence with inverse-gated decoupling at a pulse angle of 90° was used and each spectrum was averaged over 64 scans using a delay time of 10 s. The total accumulation time was approximately 12 min per spectrum.

Thermogravimetry. Dried empty silica microcapsules were heated up to 700 °C at 10 °C min^{-1} in a pure oxygen atmosphere using a TGA Q500 thermogravimetric analyzer (TA instruments). This protocol is required to minimize char formation from the biopolymer component. Almost complete pyrolysis of the chitosan and HPC located within the silica walls was achieved, leaving silica as a white residue. Chitosan, HPC and silica were also analyzed as reference materials to aid data interpretation.

Fluorescence microscopy. An oil-soluble dye (Nile Red) was added to the oil phase prior to high-shear homogenization and the resulting silica microcapsules were visualized by fluorescence microscopy using a Zeiss Axio Scope A1 microscope equipped with a Zeiss Axio ICm1 camera. Fluorescence images were recorded using an LED radiation source combined with filter set 43 HE (excitation wavelength = 550/25 nm and emission wavelength = 605/70 nm).

Analysis of pore size distribution and volume. A BET adsorption isotherm was obtained for empty silica microcapsules with a target shell thickness of 175 nm at 77 K using a Quantachrome Nova 1000e Nitrogen Sorption Analyzer. Nitrogen was used as the probe gas (area occupied per N_2 molecule = 16.2 Å^2) and the sample was degassed at 120 °C for 20 h before analysis. Adsorption data were collected at 20 points over a relative pressure range of 0.01–0.995 P/P_0. The thermal delay was set to 180 s, the equilibration time was 60 s, and the helium pumpdown time was 10 min. The specific surface area was determined using the BET equation and the mean pore radius was calculated using density functional theory (DFT) within NOVAWin software provided by the manufacturer.

Results and discussion

In an earlier study, we reported that an adsorbed layer of chitosan facilitated the surface deposition of silica onto micrometer-sized latex particles, which served as a model substrate.[61] However, this silica overlayer was generated using an ethanol-rich Stöber silica formulation.[62] Unfortunately, this well-established protocol is unsuitable for coating the droplet phase of an oil-in-water emulsion because ethanol is miscible with both phases and hence would most likely destabilize the emulsion. Instead, in the present study we examined a wholly aqueous formulation for silica deposition. In principle, this could have involved using sodium silicate as a soluble silica precursor but such formulations typically offer only poor control over silica deposition.[63,64] Of course, the hydrolysis of alternative soluble silica precursors such as TEOS or TMOS produces either ethanol or methanol as a by-product. However, if only relatively thin silica shells are targeted then the original oil-in-water emulsion should remain stable during the *in situ* silicification reaction owing to the relatively low concentration of alcohol that is present (plus its preferred location within the aqueous continuous phase).

Recently, we reported the optimization of a formulation for the preparation of oil-in-water emulsions comprising 5–10 μm diameter droplets using a binary mixture of chitosan and hydroxypropyl cellulose as an emulsifier.[60] Empirically, it was found that the finest, most stable emulsions were obtained when using a chitosan/hydroxypropyl cellulose mass ratio of 1.0 at approximately pH 4.9. Various oils were examined but the main focus of this prior study was Solvesso 200 ND – a widely used industrial oil.[65–67] According to optical microscopy and laser diffraction analysis, the volume-average oil droplet diameter could be varied from 6.6 to 42.9 μm by adjusting the stirring rate employed for high-shear homogenization. Aqueous electrophoresis studies provided evidence for adsorption of chitosan at the oil–water interface since the oil droplets exhibited positive zeta potentials at low pH.[60] Moreover, a bespoke ^{1}H NMR-based spectroscopy assay performed on the aqueous supernatant obtained after gravitational creaming of the oil droplets confirmed that both chitosan and hydroxypropyl cellulose were adsorbed at the surface of the oil droplets, with little or no evidence for preferential adsorption of either biopolymer.[60]

Initial silica microcapsule experiments

Silicification experiments were conducted using the protocol outlined in Scheme 1. Both TEOS and TMOS were employed as soluble silica precursors. TEOS is miscible with Solvesso 200 ND and was added to the oil phase prior to high-shear homogenization. TMOS, which is known to be rapidly hydrolyzed to afford water-soluble $Si(OH)_4$,[68,69] was added to the aqueous continuous phase immediately after emulsification. Thus silicification was expected to occur simultaneously at each side of the oil/water interface [N.B. One reviewer of this manuscript remarked that such silicification is not necessarily surface-confined: this is certainly true in the case of TMOS hydrolysis but TEOS hydrolysis most likely occurs solely at the oil–water interface]. Although conducted using differing silicification conditions, our prior studies[60] suggested that the cationic character of the chitosan would most likely aid surface deposition of the silica. Initially, silicification was allowed to proceed under quiescent conditions (*i.e.*, no mechanical agitation). A specimen calculation for the target silica shell thickness in such experiments – along with the various implicit assumptions that are required – is provided in the SI.

Subsequent optical microscopy studies indicated that silicification had indeed occurred. Unlike the initial perfectly spherical oil droplets, the silica microcapsules appeared to be more irregular and possess one or more dimples. Moreover, the size of the silica microcapsules was comparable to that of the original oil droplets. Hence systematic variation of the stirring rate used for high-shear homogenization when preparing

the initial oil-in-water emulsion should in principle enable the mean silica microcapsule diameter to be tuned. However, this aspect was not explored in the current study, which is focused on producing microcapsules of 5–10 μm diameter.

Laser diffraction studies indicated a $D[4,3]$ diameter of 7.1 μm for the initial oil-in-water emulsion and 8.1 μm for the final silica microcapsules, see Fig. 2. Thus, this sizing technique is consistent with the optical microscopy images shown in Fig. 1: *in situ* silicification leads to minimal change in the particle size distribution. Laser diffraction analysis also revealed the presence of a minor population of submicron-sized particles in the size distribution obtained for the silica microcapsules. In principle, this feature may correspond to either relatively small microcapsules and/or silica nanoparticles formed *via* secondary nucleation. However, a similar minor population was also observed for the initial emulsion, which suggests that the former explanation may be more likely.

The extent of silicification was studied by ^{29}Si NMR spectroscopy, which was used to monitor the reduction in the TEOS signal over time. Unfortunately, the natural abundance of ^{29}Si is only 4.7% and relatively long delay times are usually required to ensure that spin relaxation is complete between each spectrum.[70,71] This inevitably leads to low spectral resolution, long spectral acquisition times and relatively poor temporal resolution. To address these problems, an inert oil-soluble paramagnetic complex, chromium(III) acetylacetonate ($Cr(acac)_3$), was used as a paramagnetic relaxation agent. This complex has been used to monitor the kinetics of TEOS hydrolysis in the literature.[72–74]

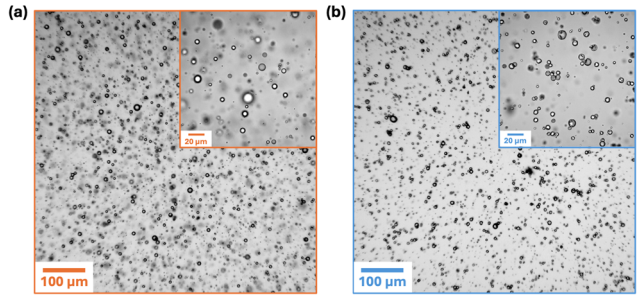

Fig. 1 Optical microscopy images recorded for: (a) a precursor oil-in-water emulsion prepared at pH 3.8 under quiescent conditions using a 0.89% w/w aqueous binary mixture of chitosan and HPC (chitosan/HPC mass ratio = 1.0) and an oil phase comprising 63% w/w Solvesso 200 ND, 7% w/w DMP and 30% w/w TEOS; (b) corresponding silica microcapsules obtained after interfacial silicification using the protocol shown in Scheme 1 (target silica shell thickness = 100 nm).

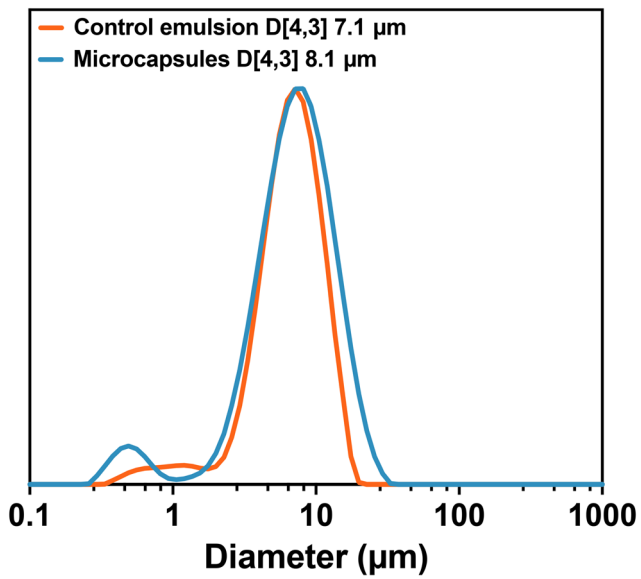

Fig. 2 Laser diffraction data recorded for: (a) a precursor oil-in-water emulsion prepared at pH 3.8 under quiescent conditions using a 0.89% w/w aqueous binary mixture of chitosan and HPC (chitosan/HPC mass ratio = 1.0) and an oil phase comprising Solvesso 200 ND, DMP and TEOS; (b) corresponding silica microcapsules obtained after interfacial silicification using the protocol shown in Scheme 1 (target silica shell thickness = 100 nm).

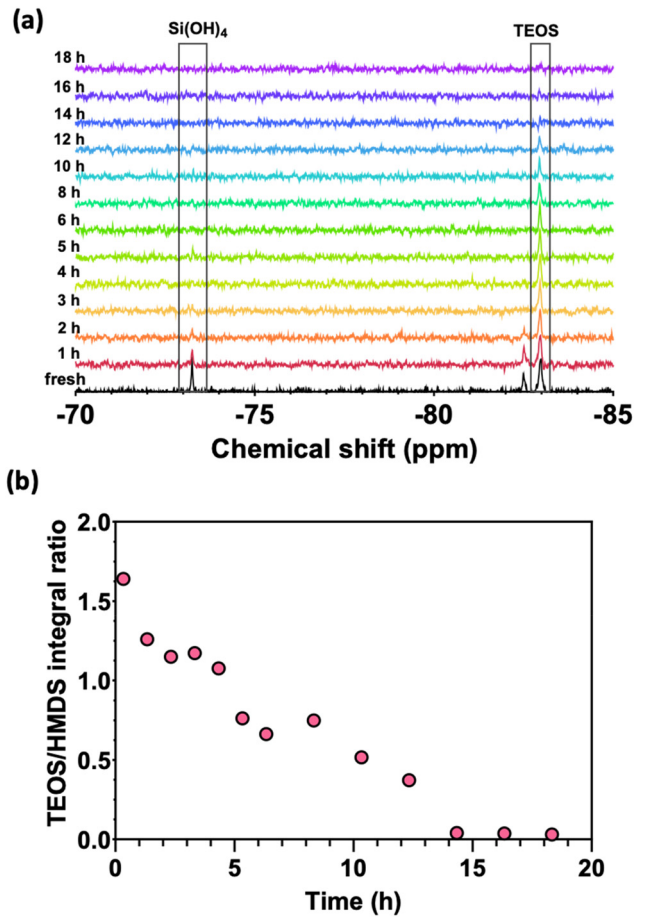

Fig. 3 Kinetics of TEOS hydrolysis within a biopolymer-stabilized oil-in-water emulsion monitored by ^{29}Si NMR spectroscopy when targeting a silica shell thickness of 100 nm using a TEOS/TMOS molar ratio of 1.0 at pH 3.8 and 20 °C. (a) Stacked ^{29}Si NMR spectra recorded over 18 h and (b) progressive attenuation of the TEOS signal (normalized with respect to hexamethyldisiloxane, HMDS) over time calculated from the spectra shown in (a).

The rates of TMOS hydrolysis and condensation are significantly faster than those for TEOS.[68,69] Unfortunately, we were unable to identify a suitable inert water-soluble paramagnetic agent for the aqueous phase, so it was not possible to monitor the TMOS reaction kinetics at 20 °C. Nevertheless, the rate of TEOS hydrolysis can be examined by monitoring the reduction in the TEOS signal (normalized with respect to HMDS; the weaker signal observed at −82.5 ppm is assigned to Si $(OEt)_3OH$[74]) at −82.9 ppm over time (see Fig. 3). Clearly, there is no unreacted TEOS remaining within the oil droplets after 15 h. However, this does not necessarily mean that all of the TEOS has been converted into silica on this time scale: see eqn (1) and (2) below for the two-stage formation of silica *via* the hydrolysis of TEOS/TMOS followed by condensation and concomitant generation of ethanol/methanol as a by-product.

$$\mathrm{Si(OR)_4} + x\mathrm{H_2O} \xrightarrow{hydrolysis} \mathrm{(OR)_{4-x}Si(OH)_x} + x\mathrm{ROH} \quad (1)$$

$$n\mathrm{(OR)_{4-x}Si(OH)_x} \xrightarrow{\text{condensation}} \mathrm{(SiO_2)_n} + \frac{nx}{2}\mathrm{H_2O} + \frac{n(4-x)}{2}\mathrm{ROH} \quad (2)$$

In a separate experiment, we attempted to monitor the kinetics of a TMOS-only silicification reaction but no ^{29}Si signals could be detected (spectra not shown). Thus, when using a TEOS/TMOS molar ratio of 1.0 for silicification, the −73.2 ppm signal assigned to $Si(OH)_4$ cannot be attributed to fully hydrolyzed TMOS. This $Si(OH)_4$ species must instead originate from TEOS hydrolysis (see eqn (1)) and most likely resides near the oil/water interface (*i.e.*, in close proximity to the oil-soluble $Cr(acac)_3$).

Table 1 Effect of varying the solution pH on silica microcapsule formation and mean diameter when targeting a silica shell thickness of 100 nm using a TEOS/TMOS molar ratio of 1.0 and a 0.89% w/w aqueous binary mixture of chitosan and HPC (chitosan/HPC mass ratio = 1.0) and reacting for 18 h without stirring at 20 °C

pH	TEOS hydrolysis within 18 h[a]?	Silica shell formation[b]?	*D*[4,3] μm	*D*[3,2] μm
2.13	Yes	No	13.9	4.2
3.65	Yes	Yes	10.2	3.4
3.82	Yes	Yes	6.2	3.4
4.08	No	Yes	6.2	3.5
4.30	No	Yes	7.8	4.2
4.92	No	Yes	9.5	4.2

[a] Based on disappearance of the TEOS signal at −82.9 ppm as judged by ^{29}Si NMR spectroscopy (Fig. S1). [b] Based on optical microscopy studies performed after 18 h.

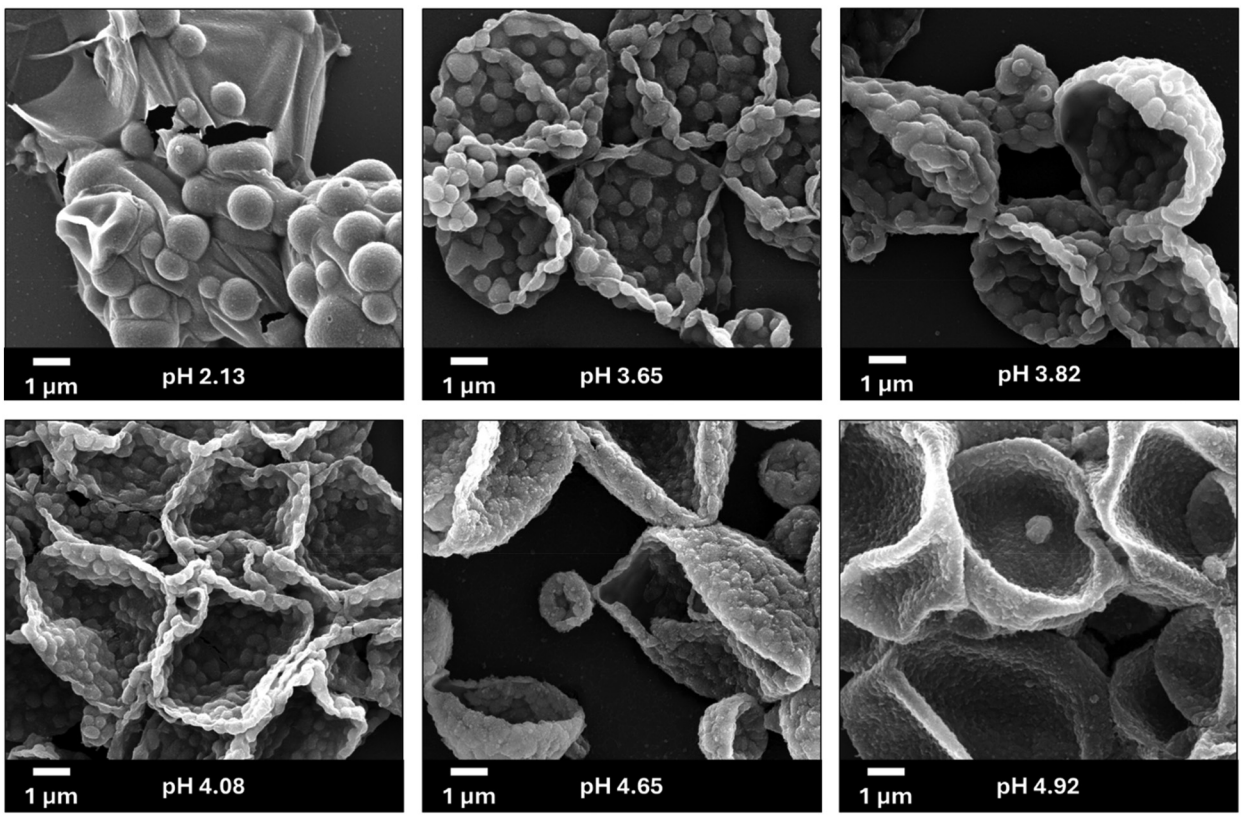

Fig. 4 Representative SEM images recorded for silica microcapsules prepared at various solution pH when targeting a mean silica shell thickness of 100 nm (see Table 1 for further details). Each synthesis utilized a TEOS/TMOS molar ratio of 1.0 and a 0.89% w/w aqueous binary mixture of chitosan and HPC (chitosan/HPC mass ratio = 1.0); silicification was conducted for 18 h without stirring at 20 °C.

Effect of varying the solution pH on silica microcapsule formation

A summary of the effect of varying the solution pH on silica microcapsule formation when targeting a silica shell thickness of 100 nm is provided in Table 1.

Inspecting Table 1, using a solution pH of either 3.65 or 3.82 is clearly optimal because such reaction conditions lead to complete TEOS hydrolysis and successful formation of silica microcapsules. Moreover, slightly smaller microcapsules were obtained at pH 3.82 compared to pH 3.65. In contrast, no silica microcapsules were obtained at pH 2.13, whereas TEOS hydrolysis remains incomplete even after 18 h above pH 4. This is consistent with a prior study of acid-catalyzed TEOS hydrolysis in which this reagent reacts significantly faster at pH 3.8 compared to pH 4.1 or pH 4.4 (albeit in the presence of ethanol cosolvent).[72] Finally, syntheses performed at 30 °C and pH 3.82 produced silica microcapsules of essentially the same size as those obtained at 20 °C.

Although the rate of TEOS hydrolysis is significantly faster below pH 3.8 (for example, it is complete within 10 h at pH 2.1), this does not necessarily mean that the condensation reaction goes to completion. This is because the fully hydrolyzed $Si(OH)_4$ species is known to be more stable at low pH.[75]

Scanning electron microscopy was used to examine the size and surface morphology of the silica microcapsules (see Fig. 4). The silica microcapsule morphology is rather ill-defined at pH 2.13, while relatively thick silica shells are formed at pH 3.65 compared to those obtained at pH 3.82. In both cases, these silica shells exhibit considerable surface roughness. Given that TMOS is hydrolyzed much more rapidly than TEOS in such formulations, these surface globules are

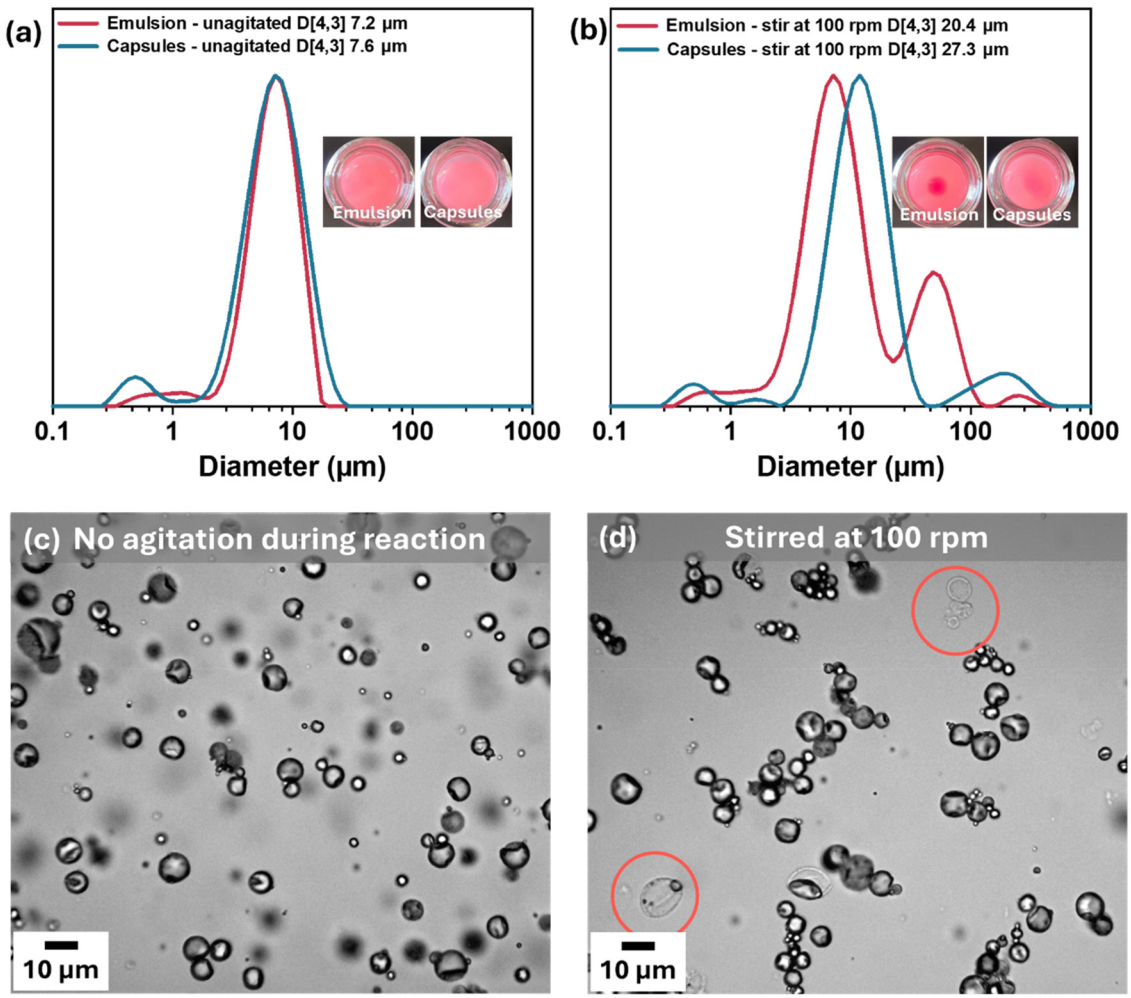

Fig. 5 Laser diffraction particle size distributions recorded for: (a) a quiescent emulsion (no stirring) and the resulting aqueous suspension of silica microcapsules, (b) an emulsion stirred at 100 rpm and the resulting aqueous suspension of silica microcapsules (inset images are 'birds-eye' digital photographs recorded for open glass vials containing either the precursor oil-in-water emulsion or the silica microcapsules). Corresponding optical microscopy images recorded after 18 h for the silica microcapsules derived from (c) a quiescent emulsion (no stirring), (d) an emulsion stirred at 100 rpm. In the latter case, red circles are used to indicate empty silica microcapsules [N.B. A hydrophobic dye (Nile Red) was added to the oil phase prior to emulsification to aid visualization of the phase-separated oil, which forms a single macroscopic droplet when silicification was attempted at a stirring rate of 100 rpm. For the silica microcapsules, the target silica shell thickness was 100 nm in each case].

likely to result from the relatively fast deposition of silica from the aqueous phase, rather than from within the oil droplets. In contrast, significantly smoother silica shells are formed at pH 4.92. Based on these SEM images, the optimal solution pH appears to be pH 3.82. This represents a compromise between reaction yield (*i.e.* TEOS conversion into silica) and the formation of well-defined silica shells (albeit with appreciable surface roughness). Unfortunately, chitosan becomes water-insoluble above approximately pH 6 so it is not possible to investigate the feasibility of preparing silica microcapsules *via* TEOS hydrolysis in alkaline media using the current protocol.[76]

At or above pH 4.9, its rate of TEOS hydrolysis is slow but its rate of condensation is fast.[69] Thus the thickest silica shells that could be targeted under such conditions was 100 nm, otherwise macroscopic gelation occurred. However, gelation could be avoided for silicification reactions conducted at pH 4.9 provided that the TEOS and/or TMOS concentrations remained below 5% w/w based on the reaction mixture. In practice, this means that targeting thicker silica shells requires more dilute reaction mixtures. Moreover, the rate of TEOS hydrolysis is relatively slow under such conditions.

Another important aspect of this interfacial silicification reaction is the effect of agitation on microcapsule formation. The effect of stirring the reaction mixture at 100 rpm is compared to using a quiescent (unstirred) reaction mixture in Fig. 5. Agitation clearly causes droplet coalescence during the early stages of the reaction, which produces both coarser droplets and a separate macroscopic oil phase. It also produces aggregated microcapsules and some capsules are clearly ruptured (Fig. 5d). Similar problems were observed when placing glass vials containing such reaction mixtures on a roller mill for even gentler agitation (see Fig. S2). In contrast, a quiescent reaction mixture produced well-dispersed microcapsules with no sign of any macroscopic phase separation of the oil phase as judged by both laser diffraction and optical microscopy analysis.

Effect of varying the chitosan/HPC mass ratio

Based on literature precedent, chitosan is considered to be the active component in terms of directing silica shell formation at the oil/water interface.[61,77,78] On the other hand, we recently found that the addition of HPC conferred some advantages in terms of emulsion droplet size and long-term stability.[60] More specifically, we found empirically that a chitosan/HPC mass ratio of 1.0 was optimal for the preparation of oil-in-water emulsions.[60] However, it was not clear whether this chitosan/HPC mass ratio would also be optimal for *in situ* silicification of the oil droplets. In the present study, we therefore also examined a chitosan/HPC mass ratio of 0.25 to provide a comparison.

In principle, aqueous electrophoresis measurements should provide useful information regarding the surface composition of both the precursor oil-in-water emulsion and the final silica microcapsules. Accordingly, zeta potential *vs.* pH curves were constructed for emulsions and microcapsules prepared when using a chitosan/HPC mass ratio of either 0.25 or 1.0, respectively (see Fig. 6). For the emulsion prepared using a chitosan/HPC mass ratio of 1.0, a relatively high zeta potential of approximately +60 mV was observed at around pH 4. There is a monotonic reduction in zeta potential at higher pH, with an isoelectric point observed at approximately pH 7.9. At higher pH, only very weakly negative zeta potentials (below −5 mV) were obtained. Thus this electrophoretic footprint pro-

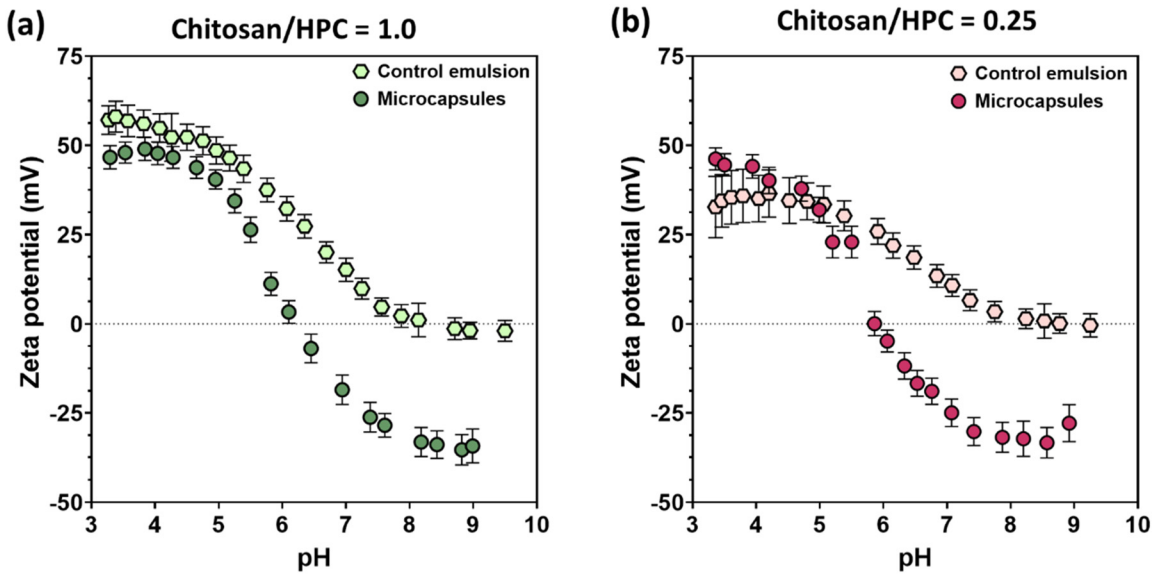

Fig. 6 Zeta potential *vs.* pH curves recorded for a precursor oil-in-water emulsion and the corresponding silica microcapsules when using a chitosan/HPC mass ratio of (a) 1.0 or (b) 0.25. The target silica shell thickness was 100 nm in each case. Conditions: 10% w/w oil; 0.89% w/w binary mixture of chitosan and HPC; TEOS/TMOS molar ratio = 1.0; pH 3.8; 20 °C.

vides strong evidence for the adsorption of chitosan at the oil/water interface. The corresponding silica microcapsules obtained when targeting a silica shell thickness of 100 nm exhibited strikingly different electrophoretic behavior. In this case, a zeta potential of around +50 mV was still observed at around pH 4 but the isoelectric point was shifted to pH 6.1. Importantly, strongly negative zeta potentials of −30 to −35 mV were obtained at pH 8–9, which is consistent with the formation of an anionic silica shell.

Given that HPC is a non-ionic water-soluble polymer, it is not surprising that reducing the chitosan/HPC mass ratio from 1.0 to 0.25 leads to significantly less positive zeta potentials being observed at pH 4 for both the precursor emulsion (+35 mV) and the corresponding silica microcapsules (+45 mV). The former system exhibited an isoelectric point at pH 8.0, while the latter had an isoelectric point at around pH 5.8. The oil droplets did not possess any anionic character even at pH 9, whereas the silica microcapsules exhibited strongly negative zeta potentials (−30 mV) above pH 8. In summary, these electrophoretic data are consistent with the successful deposition of silica shells onto the oil droplets. Given that the oil/water interface comprises a relatively thick adsorbed layer comprising both chitosan and HPC chains, this leads to the formation of an organic–inorganic nanocomposite shell. Such overlayers might be expected to exhibit significantly greater mechanical flexibility than a pure silica shell and there is some evidence that this is indeed the case (see SEM images shown in Fig. 4 and later discussion).

These two types of silica microcapsules were then purified *via* three centrifugation-redispersion cycles to remove any excess biopolymer and then subjected to gentle mechanical agitation (magnetic stirring at 130 rpm for 24 h at pH 4) to assess the structural integrity of the silica shells and their ability to retain the encapsulated oil. Laser diffraction analysis indicated that the silica microcapsules prepared using a chitosan/HPC mass ratio of 0.25 were significantly larger than those prepared using a chitosan/HPC mass ratio of 1.0 (see Fig. 7). Perhaps more importantly, optical microscopy studies suggest that a significantly higher fraction of the former microcapsules appear to be empty (*i.e.* contain no oil) after the mechanical agitation experiment.

Silicification using solely TEOS Or TMOS

The preparation of silica microcapsules was also attempted using solely TEOS (located within the oil droplets prior to high-shear homogenization) or solely TMOS (which was added to the aqueous phase immediately after high-shear homogenization). The resulting microcapsules were compared to those obtained using a TEOS/TMOS molar ratio of 1.0. Laser diffraction data are shown in Fig. 8. The particle size distribution recorded for the TMOS-only microcapsules (D[4,3] = 7.4 μm) was comparable to the droplet size distribution observed for the precursor emulsion (D[4,3] = 7.1 μm). The conventional silica microcapsules exhibited a slightly larger mean diameter of 8.1 μm. However, the TEOS-only microcapsules had a much larger apparent D[4,3] diameter of 17.2 μm. Moreover, signifi-

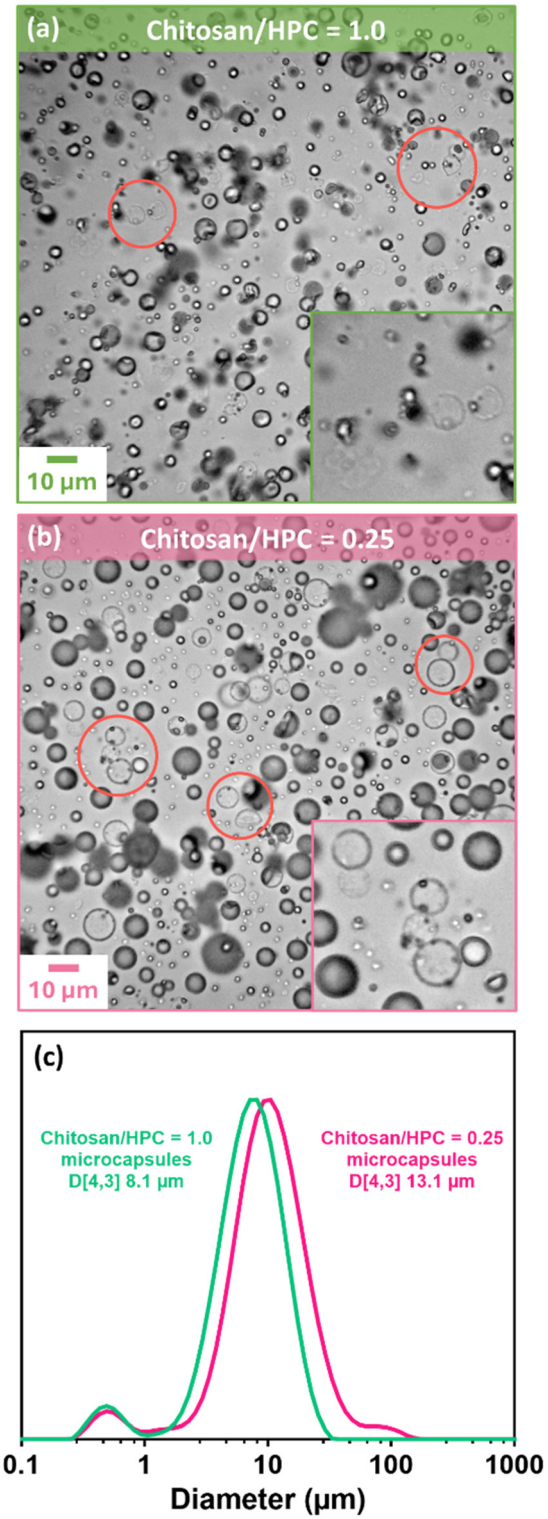

Fig. 7 Representative optical microscopy images recorded after 24 h for silica microcapsules prepared when targeting a silica shell thickness of 100 nm at pH 3.8 by magnetic stirring at 130 rpm using a chitosan/HPC mass ratio of (a) 1.0 or (b) 0.25. Conditions: 0.89% w/w biopolymer. The red circles (also see insets) indicate the formation of empty microcapsules (i.e. containing no oil). The corresponding laser diffraction particle size distributions are presented in (c).

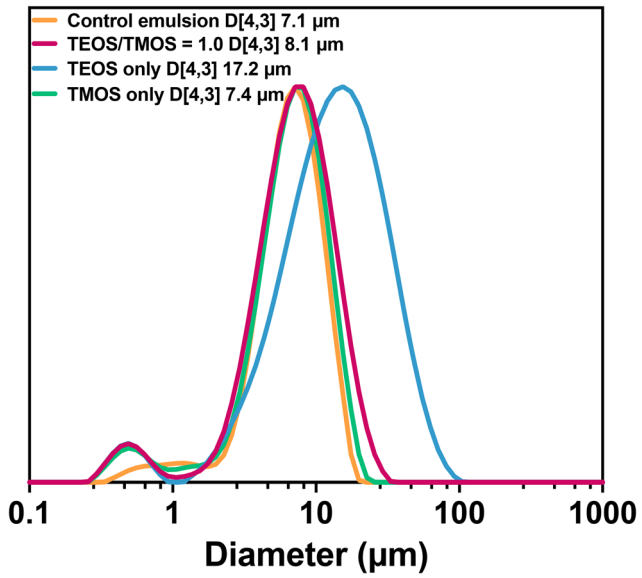

Fig. 8 Laser diffraction data obtained for silica microcapsules prepared using TEOS alone, TMOS alone or a TEOS/TMOS molar ratio of 1.0 when targeting a silica shell thickness of 100 nm in each case. Conditions: 10% w/w oil; 0.89% w/w biopolymer; chitosan/HPC mass ratio = 1.0; silicification conducted at pH 3.8 for 18 h under quiescent conditions (no stirring) at 20 °C.

cant microcapsule aggregation was observed when inspecting this aqueous suspension by optical microscopy (Fig. 9).

The effect of mechanical agitation on the structural integrity of these three types of silica microcapsules was assessed *via* optical microscopy (see Fig. 9). Some of the TMOS-only microcapsules disintegrated under such conditions (see red circles), suggesting that they are rather brittle. The TEOS-only microcapsules seem to be more flexible because most of the empty microcapsules formed in this case appear to remain intact. Finally, a few empty microcapsules were also observed for the silica microcapsules prepared using both TEOS and TMOS after 24 h of mechanical agitation. However, far more microcapsules retained their oil payload in this case. This suggests that using a combination of TEOS and TMOS for silicification produces the most resilient silica microcapsules.

SEM studies indicate that the TMOS-only silica microcapsules have distinctly globular shells (mean globule diameter = 87 ± 59 nm based on 50 measurements) while the TEOS-only silica microcapsules exhibit significantly smoother shells (see Fig. S3). This is consistent with the relatively rapid rate of TMOS hydrolysis,[69] which leads to rather poor control over the morphology of the deposited silica shells. The corresponding silica microcapsules produced using a binary mixture

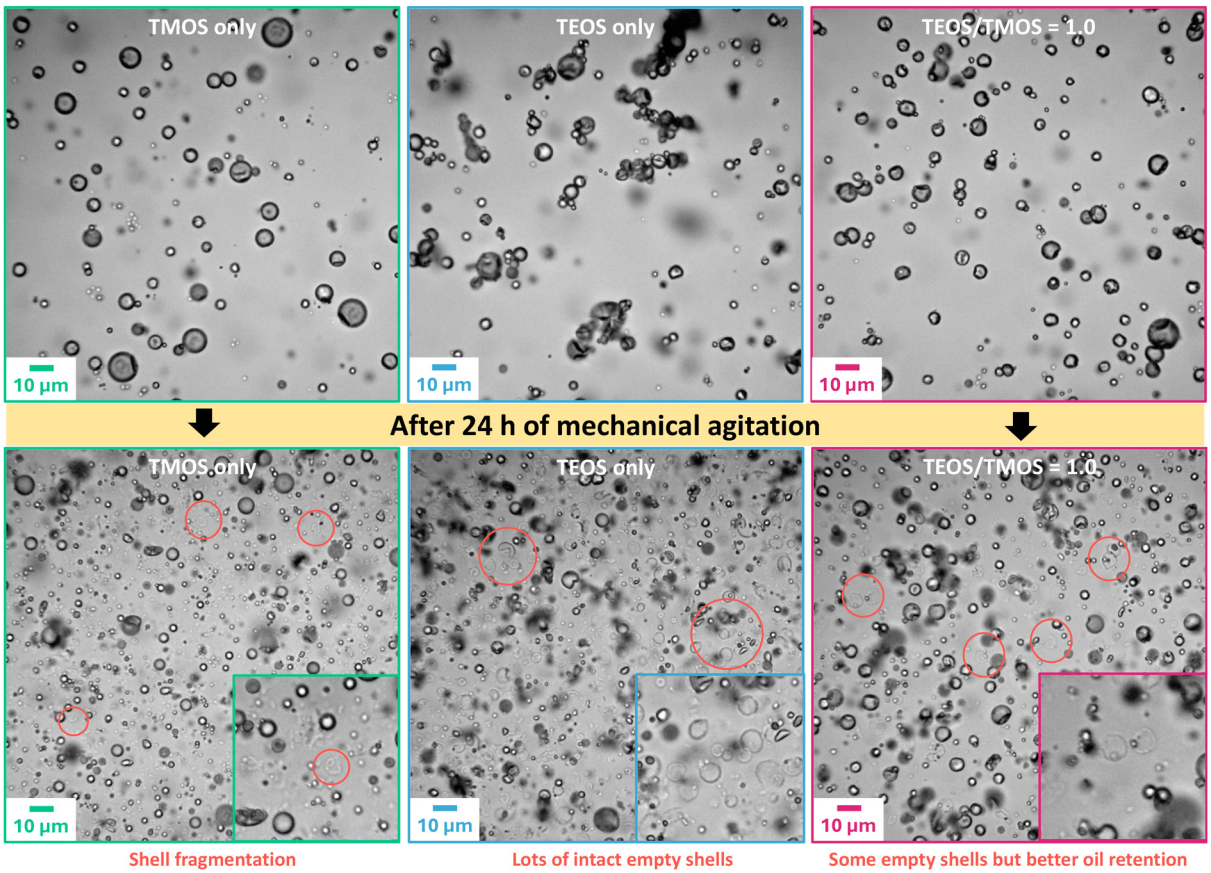

Fig. 9 Optical microscopy images recorded for three types of silica microcapsules prepared using TEOS alone, TMOS alone or a TEOS/TMOS molar ratio of 1.0 before (top row) and after (bottom row) being subjected to mechanical agitation (magnetic stirring at 130 rpm for 24 h). Conditions: 10% w/w oil; 0.89% w/w biopolymer; chitosan/HPC mass ratio = 1.0; silicification conducted at pH 3.8 for 18 h under quiescent conditions (no stirring) at 20 °C.

of TEOS and TMOS also exhibit a rather globular surface morphology but with a slightly smaller globule diameter of 79 ± 24 nm (based on 100 measurements).

Systematic variation of the oil mass fraction

Industrial applications for microcapsules require process-intensive syntheses for maximum cost efficiency. Accordingly, the synthesis of silica microcapsules targeting a silica shell thickness of 100 nm was attempted using 15%, 20%, 25% or 30% w/w oil using a TEOS/TMOS molar ratio of 1.0. For this series of experiments, the chitosan/HPC mass ratio was 1.0 and the overall biopolymer concentration was fixed at 0.80% w/w of the final emulsion. Unfortunately, reaction mixtures containing either 25% or 30% w/w oil formed gels on standing overnight, so no further analysis was performed for these failed syntheses. The 20% w/w oil formulation was very viscous, while the 15% and 10% formulations proved to be free-flowing fluids. Using the droplet size distribution of the corresponding precursor emulsion as a reference, laser diffraction data and optical microscopy images indicated that significant aggregation occurred when attempting silicification at 20% w/w oil (see Fig. 10 and 11). In summary, the upper limit oil concentration when targeting a silica shell thickness of 100 nm appears to be approximately 15% w/w. In principle, targeting thinner silica shells might enable higher oil concentrations to be achieved. Indeed, targeting a silica shell thickness of 60 nm at an oil mass fraction of 20% w/w and a TEOS/TMOS molar ratio of 1.0 also produced well-defined silica microcapsules at pH 4.9 without inducing gelation or causing aggregation (see Fig. S4).

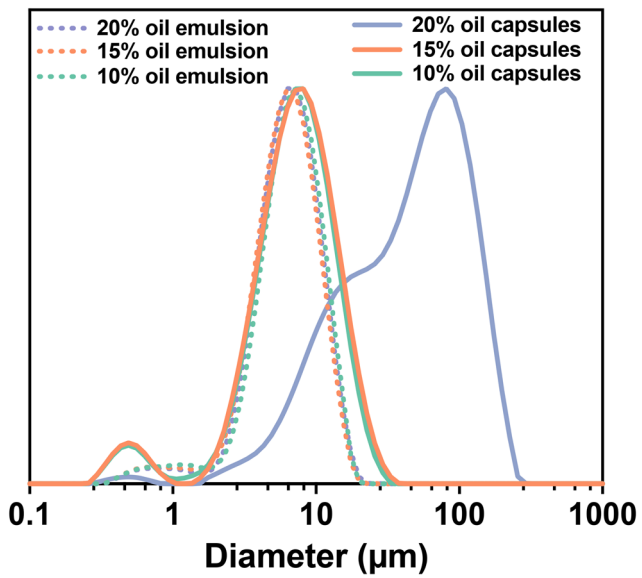

Fig. 10 Laser diffraction data comparing the droplet size distribution of each precursor emulsion to the particle size distribution of silica microcapsules prepared at varying oil mass fractions after a reaction time of 18 h. The target silica shell thickness was 100 nm in each case. Conditions: 0.80% w/w biopolymer with respect to the final emulsion; chitosan/HPC mass ratio = 1.0; TEOS/TMOS molar ratio = 1.0; pH 3.8; 20 °C; no stirring.

Effect of varying the mean silica shell thickness

The target silica shell thickness was varied from 50 nm to 200 nm using the optimized silicification conditions (*i.e.*, 0.89% w/w biopolymer; chitosan/HPC mass ratio = 1.0; TEOS/TMOS molar ratio = 1.0; pH 3.8–4.0 at 20 °C without stirring). The corresponding data are summarized in Table 2. Unfortunately, targeting a silica shell thickness of 200 nm (entry 6) produced an extremely viscous aqueous suspension of silica microcapsules. Thus, the realistic upper limit shell thickness is 175 nm, for which a free-flowing suspension was obtained. Laser diffraction analysis indicated similar microcapsule diameters for entries 1–5, while SEM studies confirmed that thicker silica shells were indeed obtained when targeting higher silica loadings (see Fig. 12). However, the estimated silica shell thicknesses are typically lower than those targeted. In principle, this could reflect experimental uncertainty in the density of the silica shells (which was assumed to be 1.93 g cm^{-3}). However, good agreement between the experi-

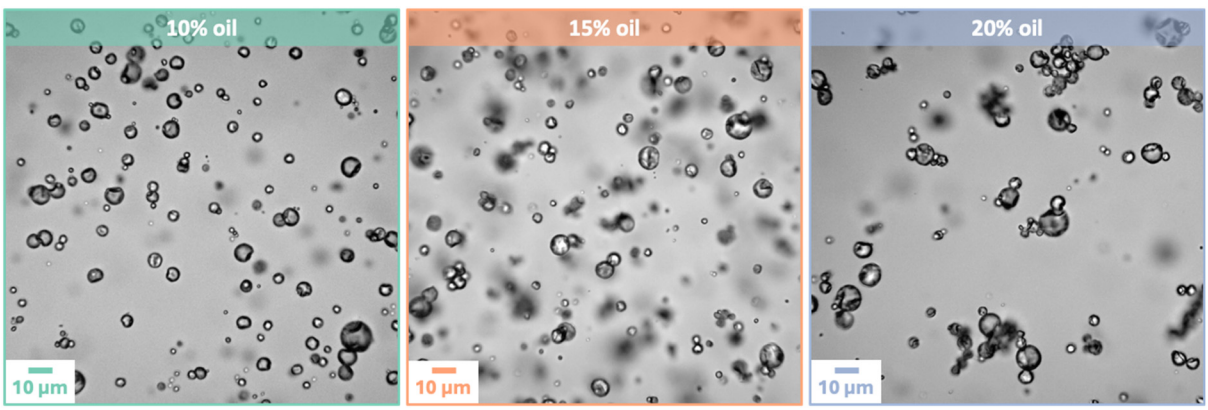

Fig. 11 Optical microscopy images recorded for silica microcapsules prepared at oil mass fractions of 10%, 15% or 20% w/w after a reaction time of 18 h. The target silica shell thickness was 100 nm in each case. Conditions: 0.80% w/w biopolymer with respect to the final emulsion; chitosan/HPC mass ratio = 1.0; TEOS/TMOS molar ratio = 1.0; pH 3.8; 20 °C; no stirring.

mental and theoretical silica shell thickness was observed when targeting the lowest silica shell thickness of 50 nm (see entry 1), which suggests that this explanation is not correct. Instead, it seems likely that either (i) the TEOS has not fully reacted or (ii) a minor fraction of the silica has formed secondary nuclei in the aqueous continuous phase, rather than being deposited at the oil/water interface.

The series of samples reported in Table 2 was subjected to thermogravimetric analysis (see Fig. 13). It is well-known that chitosan tends to form a char when heated in air.[79] However, this problem can be avoided if pyrolysis is conducted in an oxygen atmosphere.[80] Indeed, thermogravimetric analysis of both chitosan and HPC produced negligible char (<1%) when heated to 600 °C under such conditions (see Fig. S5). Thus, this protocol can be used to assess the biopolymer content of the dried silica shells. As expected, the mass% of incombustible silica remaining at 650–700 °C increases when targeting higher silica shell thicknesses owing to the lower proportion of biopolymer content in such samples. More specifically, the biopolymer content was reduced from approximately 38% for the 50 nm silica shells to around 29% for the 175 nm silica shells (Table 3).

Table 2 Laser diffraction data and silica shell thicknesses (estimated from SEM images) for silica microcapsules prepared when targeting silica shell thicknesses of 50 to 200 nm. Formulation conditions: 10% oil (10% DMP in Solvesso 200 ND), 0.89% w/w aqueous biopolymer solution comprising a chitosan/HPC mass ratio of 1.0 at pH 3.8, TEOS/TMOS molar ratio = 1.0, high-shear homogenization at 20 000 rpm for 2 min followed by silicification for 18 h without stirring at 20 °C

Target shell thickness (nm)	$D[4,3]^a$ (μm)	$D[3,2]^a$ (μm)	Estimated silica shell thickness[b] (nm)
50	7.6	4.0	51 ± 12 nm (100)[c]
100	8.1	3.9	79 ± 24 nm (100)
125	6.0	3.3	91 ± 46 nm (50)
150	6.5	3.3	131 ± 37 nm (50)
175	6.4	3.3	168 ± 91 nm (50)
200	9.4	3.9	173 ± 80 nm (30)

[a] Determined by laser diffraction. [b] Estimated by scanning electron microscopy. [c] Number of measurements made per analysis.

Preliminary release studies

DMP was used as a model compound to examine the permeability of the silica microcapsules. The aqueous solubility of DMP is approximately 4.2 g dm^{-3} (or 4200 ppm) at ambient temperature.[81] Under the conditions used for the equilibrium dialysis experiments, the maximum DMP concentration was 85–100 ppm. Thus the DMP was always present below its saturation concentration, which ensured its continuous diffusion from the dialysis tubing into the aqueous continuous phase. UV spectroscopy studies indicated a molar extinction coefficient of 1414 ± 2 dm mol^{-1} cm^{-1} for DMP (see calibration data in Fig. S6), which is close to that reported for similar compounds (*e.g.* diethyl phthalate) in the literature.[82]

The DMP release data are shown in Fig. 14. As expected, DMP diffusion from the oil droplets proceeded rapidly, with 92% release being observed within 6 h at 20 °C. Essentially the same rate of release was observed for the silica microcapsules

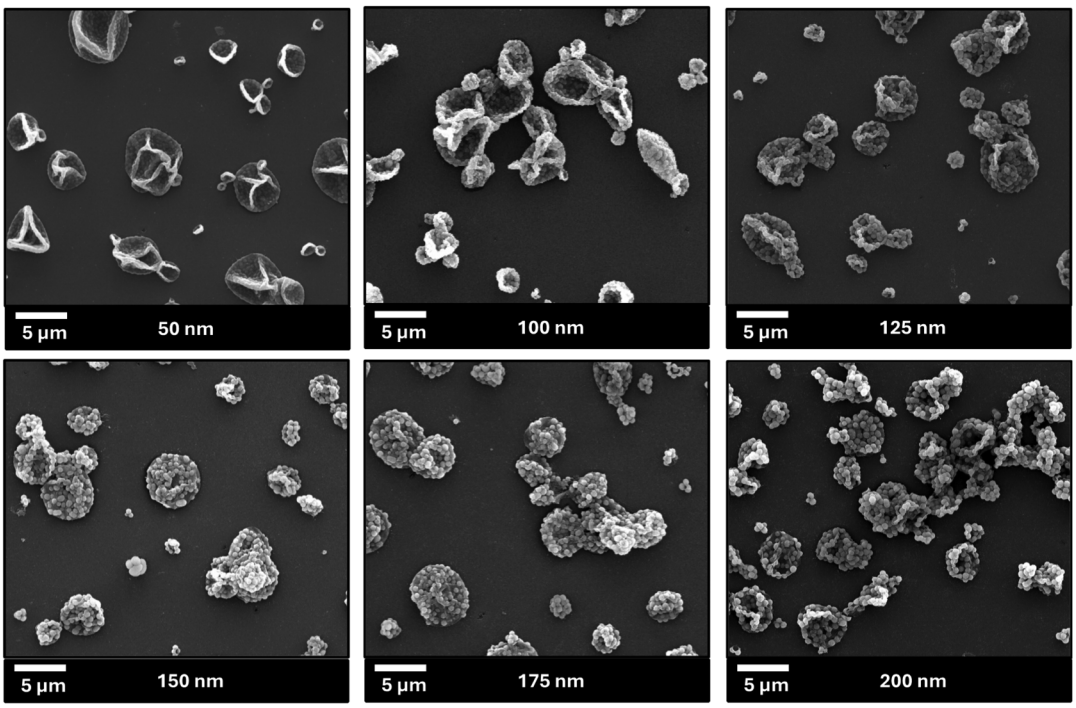

Fig. 12 Representative SEM images recorded for the silica microcapsules shown in Table 2 when targeting mean silica shell thicknesses ranging from 50 nm to 200 nm.

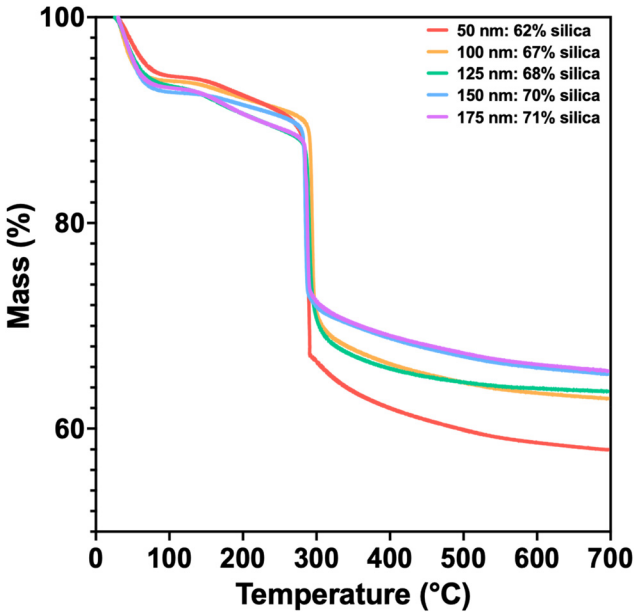

Fig. 13 Thermogravimetric analysis curves recorded under an oxygen atmosphere for five examples of silica microcapsules with target silica shell thicknesses ranging from 50 nm to 175 nm (see Table 2).

Table 3 Comparison of the calculated silica content with the actual silica content determined *via* thermogravimetry for dry biopolymer/silica composite capsules at varying shell thicknesses

Target silica shell thickness/nm	Theoretical silica content/%	Silica content by TGA[a]/%	Calculated silica yield[c]/%	Biopolymer content/%
50 nm	61	62	~100	38
100 nm	75	67	89	33
125 nm	79	68	86	32
150 nm	82	70	86	30
175 nm	84	71	84	29
Silica control	100	95[b]	95	N/A

[a] Determined by thermogravimetric analysis in an oxygen atmosphere. [b] Indicates surface moisture content. [c] Silica yields were calculated by comparing the actual and theoretical silica contents.

with a mean shell thickness of 50 nm, which indicates that this inorganic overlayer is highly permeable.

Targeting thicker silica shells led to marginally better performance: 81% DMP permeated 125 nm silica shells within 6 h while 73% DMP was released over the same time period from microcapsules comprising a silica overlayer of 175 nm. Nevertheless, these silica microcapsules are clearly highly porous and hence unable to retain sparingly water-soluble small molecules over time scales of days. Indeed, BET surface area analysis (N_2 probe gas at 77 K) of dried silica microcapsules indicated a specific surface area of 95 m^2 g^{-1} and a mean pore radius of approximately 39 Å was calculated using a density functional theory (DFT) model. The latter value is consistent with the observed rapid release of DMP and is comparable to that reported for fragrance-loaded silica microcapsules prepared using TEOS in the literature.[83] On the other hand, fluorescence microscopy studies indicate that a model highly water-insoluble dye (Nile Red) is retained within such silica microcapsules for at least sixteen weeks when stored as an aqueous suspension at 20 °C, see Fig. 15. However, it remains to be seen whether such silica microcapsules can retain payloads such as commercial fragrances – which typically comprise a range of compounds of varying hydrophobic character – over a similar time scale.

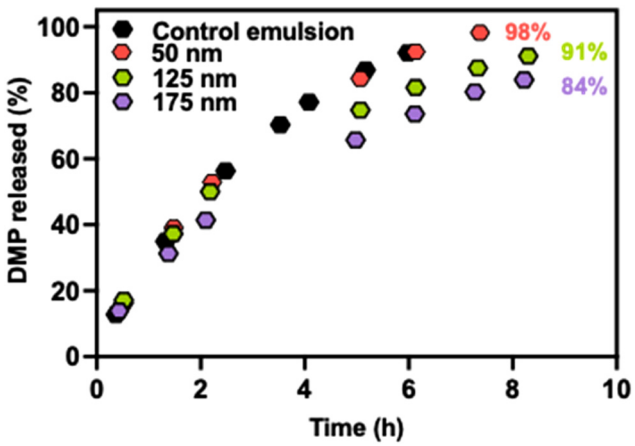

Fig. 14 Release kinetics observed for three types of silica microcapsules (mean silica shell thickness = 50, 125 or 175 nm, plus the corresponding precursor emulsion) using UV spectroscopy to monitor the diffusion of a sparingly water-soluble payload (dimethyl phthalate, DMP) at 20 °C.

In summary, the optimum reaction conditions for the preparation of silica microcapsules starting from oil-in-water emulsions prepared using a binary mixture of chitosan and HPC as an emulsifier at 20 °C are as follows. First, the emulsion should be quiescent because mechanical agitation tends to destabilize the oil droplets. Second, using a chitosan/HPC mass ratio of 1.0 tends to produce the best silica microcapsules. Third, the highest-quality silica shells are obtained when using a binary mixture of an oil-soluble silica precursor (TEOS) located within the droplet phase and TMOS within the aqueous continuous phase. The resulting silica shells are relatively flexible owing to their biopolymer content, which ranges from 38% to 29% by mass depending on the target silica shell thickness, as judged by thermogravimetric analysis. Silica shell thicknesses of approximately 50–175 nm can be achieved within 18 h at oil mass fractions of up to 0.15. Silica deposition leads to a significant shift in the isoelectric point to higher pH compared to that for the precursor oil-in-water emulsion. It is perhaps also worth emphasizing that our formulation for the preparation of silica microcapsules is much more straightforward and scalable than the rather complex multistep protocol reported by Zhang and co-workers.[8] Alternative formulations also suffer from various disadvantages, including long reaction times[51] or the use of bespoke

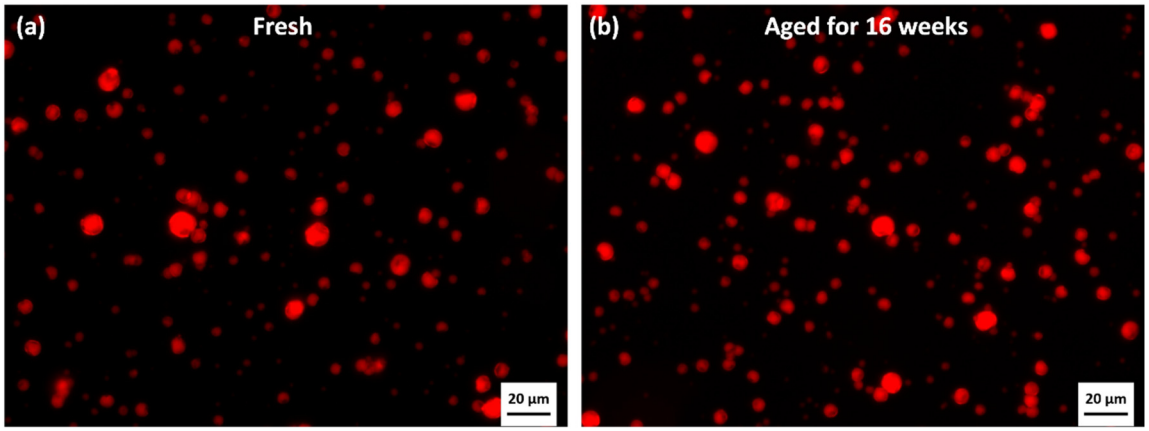

Fig. 15 Fluorescence microscopy images recorded for silica microcapsules (silica shell thickness = 100 nm) prepared using Nile Red dye dissolved in the oil phase prior to high-shear homogenization: (a) as-prepared microcapsules and (b) microcapsules aged as an aqueous suspension for sixteen weeks at 20 °C. Silicification conditions: 10% w/w oil; chitosan/HPC mass ratio = 1.0; TEOS/TMOS molar ratio = 1.0; 0.89% w/w biopolymer; pH 3.8, 20 °C.

exotic polymeric oils.[84] Given that almost all the TMOS and TEOS is converted into silica and almost all the silica is deposited onto the oil droplets, the synthesis of silica microcapsules using our new formulation proceeds with high efficiency. Current disadvantages include the generation of methanol and ethanol as by-products, the loss of control over the shell morphology when targeting thicker silica overlayers, and the use of TMOS rather than sodium silicate as the water-soluble silica precursor. A more process-intensive formulation would also be useful for potential commercial applications.

Conclusions

A new route to sustainable silica microcapsules is reported based on the judicious use of a binary mixture of chitosan and hydroxypropyl cellulose. These two biopolymers act as a synergistic emulsifier system to produce an oil-in-water emulsion with a mean droplet diameter of approximately 5–10 μm. Aqueous electrophoresis studies confirm that the oil droplets possess cationic surface charge, which indicates chitosan adsorption at the oil–water interface. This component directs the surface deposition of silica from the aqueous continuous phase when using TMOS as a soluble silica precursor. Interestingly, the best-quality microcapsules are invariably obtained when adding TEOS to the oil phase prior to high-shear homogenization. Thus the silica shells of the resulting microcapsules are formed from both sides of the oil–water interface. Moreover, the two biopolymers within these silica shells confer some degree of mechanical flexibility, which may offer a potential advantage for controlled release applications. Variation of the silica synthesis conditions enables the mean silica shell thickness to be varied from around 50 nm up to approximately 175 nm. Analysis of the dried silica shells by thermogravimetry under an oxygen atmosphere indicated a mean biopolymer content of around 38% by mass for the 50 nm silica shells, with lower contents being observed when targeting thicker silica shells. Preliminary release experiments indicate that 73–92% of a model sparingly water-soluble payload (dimethyl phthalate) is released within 6 h at 20 °C. This suggests that the silica shells are highly porous and unlikely to retain small molecules with appreciable water solubility. On the other hand, a highly hydrophobic dye such as Nile Red is retained within these silica microcapsules for at least sixteen weeks. In principle, such 'leaky' microcapsules might be useful for the sustained release of relatively hydrophobic actives such as fragrances.

Conflicts of interest

A patent application has been filed by Syngenta to protect the IP associated with this study.

Data availability

The data supporting this article have been included as part of the SI. Supplementary information: sample calculation of the mean silica shell thickness, additional ^{29}Si NMR spectra, laser diffraction particle size distributions, SEM and optical microscopy images, FT-IR spectra, thermogravimetric analysis curves for chitosan and HPC alone, and a linear calibration plot constructed using UV spectroscopy for DMP. See DOI: **https://doi.org/10.1039/d5gc03298a**.

Acknowledgements

Syngenta is thanked for funding a PhD studentship for the first author and for permission to publish this study.

References

1 W. J. Gun and A. F. Routh, Formation and characterization of pH-responsive liquid core microcapsules, *Langmuir*, 2013, **29**, 12541–12548.
2 Q. Sun, Y. Du, Z. Zhao, E. A. H. Hall, H. Gao, G. B. Sukhorukov and A. F. Routh, Functional silver-coated colloidosomes as targeted carriers for small molecules, *Langmuir*, 2017, **33**, 3755–3764.
3 Q. Sun, Z. Zhao, E. A. H. Hall and A. F. Routh, Metal coated colloidosomes as carriers for an antibiotic, *Front. Chem.*, 2018, **6**, 196.
4 T. Nomura and A. F. Routh, Benign preparation of aqueous core poly lactic-co-glycolic acid (PLGA) microcapsules, *J. Colloid Interface Sci.*, 2018, **513**, 1–9.
5 Q. Sun, Y. Du, E. A. H. Hall, D. Luo, G. B. Sukhorukov and A. F. Routh, A fabrication method of gold coated colloidosomes and their application as targeted drug carriers, *Soft Matter*, 2018, **14**, 2594–2603.
6 H. N. Yow and A. F. Routh, Release profiles of encapsulated actives from colloidosomes sintered for various durations, *Langmuir*, 2009, **25**, 159–166.
7 P. H. R. Keen, N. K. H. Slater and A. F. Routh, Encapsulation of lactic acid bacteria in colloidosomes, *Langmuir*, 2012, **28**, 16007–16014.
8 D. Baiocco, M. Al-Sharabi, B. T. Lobel, O. J. Cayre, A. F. Routh and Z. Zhang, Eco-friendly fungal chitosan-silica dual-shell microcapsules with tailored mechanical and barrier properties for potential consumer product applications, *ACS Omega*, 2024, **9**, 28385–28396.
9 J. Hu, H. Q. Chen and Z. Zhang, Mechanical properties of melamine formaldehyde microcapsules for self-healing materials, *Mater. Chem. Phys.*, 2009, **118**, 63–70.
10 Y. Long, B. Vincent, D. York, Z. Zhang and J. A. Preece, Organic–inorganic double shell composite microcapsules, *Chem. Commun.*, 2010, **46**, 1718–1720.
11 X. Pan, R. Mercadé-Prieto, D. York, J. A. Preece and Z. Zhang, Structure and mechanical properties of consumer-friendly PMMA microcapsules, *Ind. Eng. Chem. Res.*, 2013, **52**, 11253–11265.
12 D. Baiocco and Z. Zhang, Microplastic-free microcapsules to encapsulate health-promoting limonene oil, *Molecules*, 2022, **27**, 7215.
13 R. Mercadé-Prieto, R. Allen, D. York, J. A. Preece, T. E. Goodwin and Z. Zhang, Determination of the shell permeability of microcapsules with a core of oil-based active ingredient, *J. Microencapsulation*, 2012, **29**, 463–474.
14 C. T. J. Ferguson, A. A. Al-Khalaf, R. E. Isaac and O. J. Cayre, pH-responsive polymer microcapsules for targeted delivery of biomaterials to the midgut of *Drosophila suzukii*, *PLoS One*, 2018, **13**, e0201294.
15 J. P. Hitchcock, A. L. Tasker, E. A. Baxter, S. Biggs and O. J. Cayre, Long-term retention of small, volatile molecular species within metallic microcapsules, *ACS Appl. Mater. Interfaces*, 2015, **7**, 14808–14815.
16 A. L. Tasker, J. P. Hitchcock, L. He, E. A. Baxter, S. Biggs and O. J. Cayre, The effect of surfactant chain length on the morphology of poly(methyl methacrylate) microcapsules for fragrance oil encapsulation, *J. Colloid Interface Sci.*, 2016, **484**, 10–16.
17 K. Stark, J. P. Hitchcock, A. Fiaz, A. L. White, E. A. Baxter, S. Biggs, J. R. McLaughlan, S. Freear and O. J. Cayre, Encapsulation of emulsion droplets with metal shells for subsequent remote, triggered release, *ACS Appl. Mater. Interfaces*, 2019, **11**, 12272–12282.
18 K. Mitchell, A. Neville, G. M. Walker, M. R. Sutton and O. J. Cayre, Synthesis and tribological testing of poly (methyl methacrylate) particles containing encapsulated organic friction modifier, *Tribol. Int.*, 2018, **124**, 124–133.
19 D. Baiocco, B. T. Lobel, M. Al-Sharabi, O. J. Cayre, A. F. Routh and Z. Zhang, Environmentally friendly calcium carbonate-polydopamine microcapsules with superior mechanical, barrier, and adhesive properties, *Sustainable Mater. Technol.*, 2024, **41**, e01001.
20 B. T. Lobel, D. Baiocco, M. Al-Sharabi, A. F. Routh, Z. Zhang and O. J. Cayre, Current challenges in microcapsule designs and microencapsulation processes: a review, *ACS Appl. Mater. Interfaces*, 2024, **16**, 40326–40355.
21 V. Eriksson, J. Mistral, T. Yang Nilsson, M. Andersson Trojer and L. Evenäs, Microcapsule functionalization enables rate-determining release from cellulose nonwovens for long-term performance, *J. Mater. Chem. B*, 2023, **11**, 2693–2699.
22 C.-H. Xue, L.-Y. Deng, S.-T. Jia and P.-B. Wei, Fabrication of superhydrophobic aromatic cotton fabrics, *RSC Adv.*, 2016, **6**, 107364.
23 H. Lai, Y. Liu, G. Huang, Y. Chen, Y. Song, Y. Q. Ma and P. Yue, Fabrication and antibacterial evaluation of peppermint oil-loaded composite microcapsules by chitosan-decorated silica nanoparticles stabilized Pickering emulsion templating, *Int. J. Biol. Macromol.*, 2021, **183**, 2314–2325.
24 X. Yang, Y. Liu, Z. Lv, Q. Hua, L. Liu, B. Wang and J. Tang, Synthesis of high latent heat lauric acid/silica microcapsules by interfacial polymerization method for thermal energy storage, *J. Energy Storage*, 2021, **33**, 102059.
25 S. Liang, Q. Li, Y. Zhu, K. Chen, C. Tian, J. Wang and R. Bai, Nanoencapsulation of n-octadecane phase change material with silica shell through interfacial hydrolysis and polycondensation in miniemulsion, *Energy*, 2015, **93**, 1684–1692.
26 Y. Huang, A. Stonehouse and C. Abeykoon, Encapsulation methods for phase change materials – a critical review, *Int. J. Heat Mass Transfer*, 2023, **200**, 123458.
27 S. Ishak, S. Mandal, H. S. Lee and J. K. Singh, Effect of core-shell ratio on the thermal energy storage capacity of SiO_2 encapsulated lauric acid, *J. Energy Storage*, 2021, **42**, 103029.
28 H. Zhang, X. Wang and D. Wu, Silica encapsulation of n-octadecane via sol–gel process: a novel microencapsulated phase-change material with enhanced thermal con-

ductivity and performance, *J. Colloid Interface Sci.*, 2010, **343**, 246–255.
29 J. Li, A. P. Hitchcock, H. D. H. Stöver and I. Shirley, A new approach to studying microcapsule wall growth mechanisms, *Macromolecules*, 2009, **42**, 2428–2432.
30 C. Ramarao, S. V. Ley, S. C. Smith, I. M. Shirley and N. DeAlmeida, Encapsulation of palladium in polyurea microcapsules, *Chem. Commun.*, 2002, **10**, 1132–1133.
31 A. Limer, F. Gayet, N. Jagielski, A. Heming, I. Shirley and D. M. Haddleton, Synthesis of microcapsules via reactive surfactants, *Soft Matter*, 2011, **7**, 5408–5416.
32 S. K. Yadav, A. K. Suresh and K. C. Khilar, Microencapsulation in polyurea shell by interfacial polycondensation, *AIChE J.*, 1990, **36**, 431–438.
33 H. B. Scher, M. Rodson and K.-S. Lee, Microencapsulation of pesticides by interfacial polymerization utilizing isocyanate or aminoplast chemistry, *Pestic. Sci.*, 1978, **54**, 394–400.
34 M. Jonsson, O. Nordin, A. L. Kron and E. Malmström, Thermally expandable microspheres with excellent expansion characteristics at high temperature, *J. Appl. Polym. Sci.*, 2010, **117**, 384–392.
35 M. Mousa, M. Jonsson, L. Granbom, A. Larsson Kron and E. Malmström, Thermally expandable microspheres based on fully or partially bio-based polymers, *J. Appl. Polym. Sci.*, 2024, **141**, e55368.
36 M. Jonsson, O. Nordin and E. Malmström, Increased onset temperature of expansion in thermally expandable microspheres through combination of crosslinking agents, *J. Appl. Polym. Sci.*, 2011, **121**, 369–375.
37 P. J. Dowding, R. Atkin, B. Vincent and P. Bouillot, Oil core-polymer shell microcapsules prepared by internal phase separation from emulsion droplets. I: Characterization and release rates for microcapsules with polystyrene shells, *Langmuir*, 2004, **20**, 11374–11379.
38 P. J. Dowding, R. Atkin, B. Vincent and P. Bouillot, Oil core/polymer shell microcapsules by internal phase separation from emulsion droplets. II: controlling the release profile of active molecules, *Langmuir*, 2005, **21**, 5278–5284.
39 A. Loxley and B. Vincent, Preparation of poly(methyl methacrylate) microcapsules with liquid cores, *J. Colloid Interface Sci.*, 1998, **208**, 49–62.
40 European Chemicals Agency, Microplastics, **https://echa.europa.eu/hot-topics/microplastics** (accessed Aug 4, 2025).
41 D. Baiocco, B. T. Lobel, M. Al-Sharabi, O. J. Cayre, A. F. Routh and Z. Zhang, Organic-inorganic multilayer microcarriers with superior mechanical properties for potential active delivery in fast-moving consumer goods, *Ind. Eng. Chem. Res.*, 2025, **64**, 4917–4931.
42 G. L. Lecomte-Nana, V. Niknam, A. Aimable, M. Bieniab, D. Kpogbemabou, J.-C. Robert-Arnouila and A. Lajmi, Microcapsules from Pickering emulsions stabilized by clay particles, in *Advances in Bioceramics and Porous Ceramics VIII*, ed. R. J. Narayan and P. Colombo, The American Ceramic Society, 2015, pp. 107–124.
43 S. A. F. Bon and T. Chen, Pickering stabilization as a tool in the fabrication of complex nanopatterned silica microcapsules, *Langmuir*, 2007, **23**, 9527–9530.
44 M. Williams, S. P. Armes and D. W. York, Clay-based colloidosomes, *Langmuir*, 2012, **28**, 1142–1148.
45 R. Vecchione, G. Luciani, V. Calcagno, A. Jakhmola, B. Silvestri, D. Guarnieri, V. Belli, A. Costantini and P. A. Netti, Multilayered silica-biopolymer nanocapsules with a hydrophobic core and a hydrophilic tunable shell thickness, *Nanoscale*, 2016, **8**, 8798–8809.
46 F. He, X. Wang and D. Wu, New approach for sol–gel synthesis of microencapsulated n-octadecane phase change material with silica wall using sodium silicate precursor, *Energy*, 2014, **67**, 223–233.
47 M. Graham and D. Shchukin, Formation mechanism of multipurpose silica nanocapsules, *Langmuir*, 2021, **37**, 918–927.
48 H. Y. Kang and H. H. Chen, Preparation of thermally stable microcapsules with a chitosan–silica hybrid, *J. Food Sci.*, 2014, **79**, 1713–1721.
49 M. Sciortino, A. Scurria, C. Lino, M. Pagliaro, F. D'Agostino, S. Tortorici, M. Ricupero, A. Biondi, L. Zappalà and R. Ciriminna, Silica-microencapsulated orange oil for sustainable pest control, *Adv. Sustainable Syst.*, 2021, **5**, 2000280.
50 K. Chen, C. Xu, J. Zhou, R. Zhao, Q. Gao and C. Wang, Multifunctional fabric coatings with slow-releasing fragrance and UV resistant properties from ethyl cellulose/silica hybrid microcapsules, *Carbohydr. Polym.*, 2020, **232**, 115821.
51 J. Yeom, W. S. Shim and N. G. Kang, Eco-friendly silica microcapsules with improved fragrance retention, *Appl. Sci.*, 2022, **12**, 6759.
52 M. Al-Sharabi, B. T. Lobel, D. Baiocco, O. J. Cayre, Z. Zhang and A. F. Routh, Multicore silica microcapsules containing α-tocopherol for potential consumer product applications, *Mater. Adv.*, 2025, **6**, 1468–1477.
53 R. Mercadé-Prieto, X. Pan, A. Fernández-González, Z. Zhang and S. Bakalis, Quantification of microcapsules deposited in cotton fabrics before and after abrasion using fluorescence microscopy, *Ind. Eng. Chem. Res.*, 2012, **51**, 16741–16749.
54 M. Arruebo, M. Galán, N. Navascués, C. Téllez, C. Marquina, M. Ricardo Ibarra and J. Santamaría, Development of magnetic nanostructured silica-based materials as potential vectors for drug-delivery applications, *Chem. Mater.*, 2006, **18**, 1911–1919.
55 J. Yang, J. Lee, J. Kang, K. Lee, J. S. Suh, H. G. Yoon, Y. M. Huh and S. Haam, Hollow silica nanocontainers as drug delivery vehicles, *Langmuir*, 2008, **24**, 3417–3421.
56 S. Paneliya, S. Khanna, Ustav, A. P. Singh, Y. K. Patel, A. Vanpariya, N. H. Makani, R. Banerjee and I. Mukhopadhyay, Core shell paraffin/silica nanocomposite: a promising phase change material for thermal energy storage, *Renewable Energy*, 2021, **167**, 591–599.

57 S. Ju, Y. Miao, L. Wang, J. Shi, F. Wang, Z. Liu and J. Jiang, Development of octadecane/silica phase change nanocapsules for enhancing the thermal storage capacity of cement-based materials, *J. Energy Storage*, 2024, **89**, 111636.

58 S. He, W. Zhang, D. Li, P. Li, Y. Zhu, M. Ao, J. Li and Y. Cao, Preparation and characterization of double-shelled avermectin microcapsules based on copolymer matrix of silica–glutaraldehyde–chitosan, *J. Mater. Chem. B*, 2013, **1**, 1270–1278.

59 J. Brahms, R. Gabbard, F. Geng, J. A. Wireland, L. Xu and L. M. Popplewell, *Silica microcapsules and methods of preparing the same, International Flavors & Fragrances Inc*, WO2017161364, 2017.

60 O. Norvilaite, *Sustainable inorganic microcapsules for agrochemical applications*, PhD Thesis, University of Sheffield, 2025.

61 O. Norvilaite, C. Lindsay, P. Taylor and S. P. Armes, Silica-coated micrometer-sized latex particles, *Langmuir*, 2023, **39**, 5169–5178.

62 W. Stöber, A. Fink and E. Bohn, Controlled growth of monodisperse silica spheres in the micron size range, *J. Colloid Interface Sci.*, 1968, **26**, 62–69.

63 H. Zou and H. Schlaad, Sodium silicate route to coat polymer particles with silica, *Colloid Polym. Sci.*, 2014, **292**, 1693–1700.

64 T. Ung, L. M. Liz-Marzán and P. Mulvaney, Controlled method for silica coating of silver colloids. Influence of coating on the rate of chemical reactions, *Langmuir*, 1998, **14**, 3740–3748.

65 Solvesso 200ND is a naphthalene-depleted aromatic solvent, which is a by-product produced during crude oil distillation. Comprising mainly methyl isomers of naphthalene, it is widely used as a solvent for agricultural formulations owing to (i) its low aqueous solubility, which favours the formation of stable emulsions, (ii) its aromatic character, which enables dissolution of many agricultural active ingredients (unlike aliphatic solvents) and (iii) its crop safety, with minimal or no leaf damage being observed when applied. Moreover, Solvesso 200ND has low volatility, a relatively high boiling point (~200 °C) and a high flash point (100 °C), which are beneficial in terms of its safe handling and storage.

66 A. Christie, C. I. Lindsay and S. Gellatly, *Process for preparing microcapsules, Syngenta Crop Protection AG*, WO/2022/128680, 2022.

67 P. Taylor and C. I. Lindsay, *Microencapsulation, Syngenta Crop Protection AG*, WO/2023/061901, 2023.

68 T. N. M. Bernards, M. J. van Bommel and A. H. Boonstra, Hydrolysis-condensation processes of the tetra-alkoxysilanes TPOS, TEOS and TMOS in some alcoholic solvents, *J. Non-Cryst. Solids*, 1991, **134**, 1–13.

69 A. A. Issa and A. S. Luyt, Kinetics of alkoxysilanes and organoalkoxysilanes polymerization: a review, *Polymers*, 2019, **11**, 537.

70 K. M. Delak, T. C. Farrar and N. Sahai, ^{29}Si NMR sensitivity enhancement methods for the quantitative study of organosilicate hydrolysis and condensation, *J. Non-Cryst. Solids*, 2005, **351**, 2244–2250.

71 W. J. Malfait, W. E. Halter and R. Verel, ^{29}Si NMR spectroscopy of silica glass: T_1 relaxation and constraints on the Si–O–Si bond angle distribution, *Chem. Geol.*, 2008, **256**, 269–277.

72 J. C. Echeverría, P. Moriones, G. Arzamendi, J. J. Garrido, M. J. Gil, A. Cornejo and V. Martínez-Merino, Kinetics of the acid-catalyzed hydrolysis of tetraethoxysilane (TEOS) by ^{29}Si NMR spectroscopy and mathematical modelling, *J. Sol-Gel Sci. Technol.*, 2018, **86**, 316–328.

73 C. A. Fyfe and P. P. Aroca, Quantitative kinetic analysis by high-resolution ^{29}Si NMR spectroscopy of the initial stages in the sol-gel formation of silica gel from tetraethoxysilane, *Chem. Mater.*, 1995, **7**, 1800–1806.

74 Y. Xu, D. Wu, Y. Sun, H. Gao, H. Yuan and F. Deng, A new study on the kinetics of Stöber synthesis by *in situ* liquid ^{29}Si NMR, *J. Sol-Gel Sci. Technol.*, 2007, **42**, 13–20.

75 G. R. Choppin, P. Pathak and P. Thakur, Polymerization and complexation behavior of silicic acid: a review, *Main Group Met. Chem.*, 2008, **31**, 53–71.

76 H. Liu, C. Wang, S. Zou, Z. Wei and Z. Tong, Simple, reversible emulsion system switched by pH on the basis of chitosan without any hydrophobic modification, *Langmuir*, 2012, **28**, 11017–11024.

77 J. S. Chang, Z. L. Kong, D. F. Hwang and K. L. B. Chang, Chitosan-catalyzed aggregation during the biomimetic synthesis of silica nanoparticles, *Chem. Mater.*, 2006, **18**, 702–707.

78 B. Yu, T. Chen, F. Yang, W. Liu, Y. H. Li and W. Zheng, Chitosan as morphology-directing agent for the preparation of multiarmed selenium/carbon coaxial nanorods, *Chem. Lett.*, 2011, **40**, 242–243.

79 D. de Britto and S. P. Campana-Filho, Kinetics of the thermal degradation of chitosan, *Thermochim. Acta*, 2007, **465**, 73–82.

80 J. Zawadzki and H. Kaczmarek, Thermal treatment of chitosan in various conditions, *Carbohydr. Polym.*, 2010, **80**, 394–400.

81 J. W. McBain and H. McHan, Soap micelles that solubilize dimethyl phthalate, a liquid insoluble in water and in hydrocarbon, *J. Am. Chem. Soc.*, 1948, **70**, 3838–3840.

82 M. Taniguchi and J. S. Lindsey, Database of absorption and fluorescence spectra of >300 common compounds for use in PhotochemCAD, *Photochem. Photobiol.*, 2018, **94**, 290–327.

83 J. Yeom, M. Kang, A. Goh, J. Jeon, W. S. Shim and N. G. Kang, Timed-release silica microcapsules for consistent fragrance release in topical formulations, *Appl. Sci.*, 2024, **14**, 11308.

84 M. O'Sullivan, Z. Zhang and B. Vincent, Silica-shell/oil-core microcapsules with controlled shell thickness and their breakage stress, *Langmuir*, 2009, **25**, 7962–7966.